Mihailo Čubrović

Physical Characteristics and Photomorphographic Shape Analysis of Asteroid 3 Juno

A model of 3 Juno obtained from photometry in optical spectrum is presented. Modelling has been done using the photomorphographical method (Kaasalainen, Lamberg, Lumme, Bowell 1992). This method makes use of lightcurves from different oppositions. Description of shape is based on a mathematical model of the asteroidal surface which uses standard formalism of differential geometry. Reflection of light is described by means of some well known scattering laws (Lumme-Bowell law, Lommel-Seeliger law, etc.). Unlike the original method, in this paper mathematical and numerical techniques which allow some local concavities to be restored are used. Albedo variegations are also discussed but these results are much less reliable that the shape solution. Calculations of the shape parameters are based on inversion. In this paper a modified version of the maximum enthropy method is used, which allows good control of the stability and is more suitable for this problem than the usual statistical inversion techniques. The starting guess for the inversion was an ellipsoidal model obtained from a combination of classical amplitude-aspect methods. The resulting shape of Juno shows somewhat larger irregularities than it is usual for such large asteroids. The shape, together with the albedo map, indicates that some collisional structures might exist on the surface.

1. Introduction

Modelling of asteroids is an attractive field in planetary astronomy today, containing some still unsolved problems. The only available informations about the physical characteristics of asteroids are the photometrical lightcurves and some special events (e.g. occultations), which are too rare to rely on, and non-optical observations, which are still expensive and thus available for a small portion of the asteroid population. Calculation of shape parameters from the lightcurves is a difficult problem, unsolved in the most general case. Namely, a purely theoretical discussion of this topic can be found in an early work (Russell 1906). However, further development

Mihailo Čubrović (1985), Beograd, Miroslava Jovanovića 7/2, Mathematical High School Belgrade

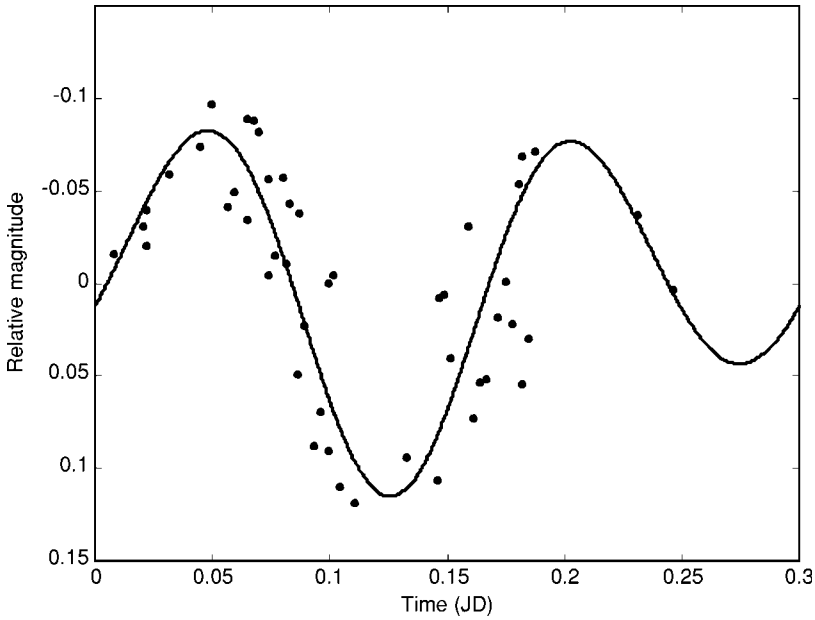

Figure 1.
Lightcurve 15 in R band

Slika 1.
Kriva 15 u R opsegu

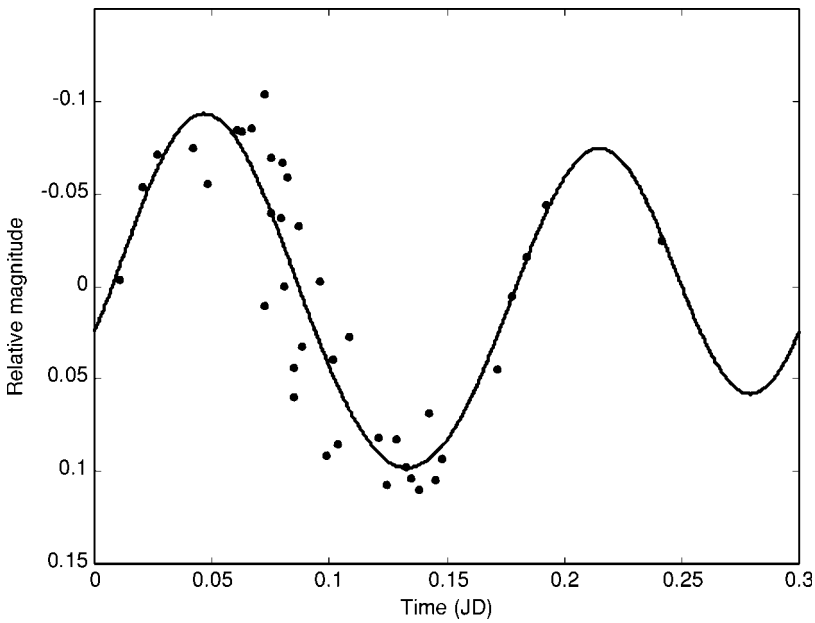

Figure 2.
Lightcurve 15 in I band

Slika 2.
Kriva 15 u I opsegu

of Russell's method started much later, in the early 1990s. The methods used for modelling thus far required many a priori assumptions and limitations, which had substantially lowered the quality and usefulness of such models. However, primarily due to its simplicity, such methods are still widely used. In this paper, as the first step, a modelling procedure also using one of

such methods (amplitude-aspect method), although combined with a more recent and more general technique (the spherical harmonics method, proposed in Lumme, Karttunen, Bowell 1989) was carried out (hereafter this procedure will be called "AAS method"). The pole solution should be as independent from the model as possible, because, obviously, the actual shape can be different from the calculated one (this is especially characteristic for ellipsoidal models). The most important feature of the spherical harmonics method is that it is not model dependent.

The first method which has allowed modelling of arbitrary shapes using the Russell's formalism is the photomorphographical method, given in Kaasalainen, Lamberg, Lumme, Bowell 1992. This method allows the shapes of asteroids to be modelled in great detail, the only limiting factor being, in theory (and, according to this paper, also in practice), the number and quality of the lightcurves used.

The lightcurve from July 2000 (published for the first time) is presented in the second section; great effort has been made to make any further analysis or use for future projects as easy as possible. The third section gives some necessary details about the old lightcurves used in this paper. The next four sections describe the methodology: in the fourth section the method for preliminary period determination is given, in the fifth section the qualitative analysis of lightcurves and analysis of the colour index curve, the sixth section describes the AAS method and in the seventh section the necessary formalism of the photomorphographic method is presented. The eighth section contains the results and some conclusions about Juno and its characteristics. In the ninth section a brief discussion of the methods used is given.

2. The New Lightcurve (July 26th-28th 2000)

The observations were done in Petnica Science Center during two consecutive nights, 26/27 and 27/28. The instruments used were the refractor telescope MEADE 178/1600 and the CCD Santa Barbara Instrument Group ST-7. Exposition lengths were 7s-10s. The observations were done in R band (660 nm) and in I band (800 nm). Only the observations in R band were included in the modelling procedure because most observations available in photometric catalogues are done in V or R band; therefore the introduction of the lightcurve in I band would unnecessarily lead to more systematic errors (without providing new information because the observing geometries are the same). The I band lightcurve is given here only to enable its use for some future analysis, by other authors.

Photometrical measurements and noise procession were done in the FITS Pro package. The magnitude of Juno was calculated by means of differential photometry, HD204391 being the comparison star. Tables 1-2 contain the data

on the observing geometry of Juno and on the comparison star. The ephemerides were calculated by the International Minor Planet Center Ephemeris Generator, and the position and the brightness of the comparison star were taken from the Tycho-2 star catalogue. The average magnitude uncertainty of the lightcurve points is 0.02*;* different points have different uncertainties.

Table 1. Equatorial and ecliptic coordinates, phase angle, elongation, and distances from the Sun and from the Earth of Juno, July 26th-28th 2000.

Date (12hUT)	RA (h)	Dec (°)	λ(°)	β(°)	α(°)	E (°)	Δ(AU)	r (AU)
26. 07.	21.49	–02.6	323.9	11.6	8.8	156.3	1.679	2.642
27. 07.	21.48	–02.7	323.6	11.6	8.5	157.3	1.672	2.639
28. 07.	21.46	–02.7	323.4	11.6	8.1	158.4	1.665	2.637

Table 2. Equatorial coordinates and VRI magnitudes for the comparison star HD 204391.

RA (h)	Dec (°)	V	R	I
21.47	–02.6	7.55	6.57	5.86

The composite lightcurves (hereafter lightcurves number 15; see the next section) are given in Figures 1 and 2. The changes of the phase angle were approximated with a linear trend. All the observations were reduced to the observational geometry of the first day of observations. The lightcurve in R band was fit simultaneously with the other lightcurves to a Fourier series with four harmonics, thus simultaneously calculating the Fourier coefficients and the period. The details of this procedure are given in the fourth section; lightcurves 15 are given in this, separate section only for the convinience of those who may want to only use the lightcurve from this paper for their research.

The I band lightcurve 15 was fit separately, using the period calculated during the simultaneous fitting of the other lightcurves (using the obvious fact that the period does not depend on the spectral band). Tables 3-4 contain the data on maxima and minima of the lightcurves. It must be stressed that, as mentioned in the previous section, the uncertainties are not the same for all points; therefore different points had different weights during the fitting procedure, so the lightcurves may seem to not be the best fit, which is because the fit is weighted.

The Fourrier coefficients for curve 15 in both bands are given in Table 5.

Table 3. Moments and relative magnitudes for extreme points of the lightcurve 15 in R band. The errors are: 0.002 for moments of maxima and minima, 0.03 for relative magnitudes.

	Maximum 1	Minimum 1	Maximum 2	Minimum 2
Time	0.048	0.126	0.202	0.275
Relative magnitude	-0.09	0.12	-0.08	0.04

Table 4. Moments and relative magnitudes of extreme points of the lightcurve 15 in I band. The errors are: 0.002 for moments of maxima and minima, 0.03 for their relative magnitudes.

	Maximum 1	Minimum 1
Time	0.047	0.133
Relative magnitude	–0.08	0.10

Table 5. Fourier coefficients of the lightcurve 15.

R band	–0.0280	0.0127	0.0403	–0.0683	–0.0001	0.0052	0.0002	0.0001
I band	–0.0323	0.0028	0.0538	–0.0562	0.0031	–0.0104	0.0002	0.0000

3. Lightcurves Used for Modelling

All the old lightcurves were taken from the Uppsala Photometric Catalogue of Asteroids. This catalogue contains magnitudes, observing geometries and references for published lightcurves up to the year 1995. Those lightcurves which did not cover at least one half of the period, as well as those which had (or seemed to have) magnitude uncertainties larger than 0.03 were discarded. The lightcurves that seemed to affect the period value too much and those which substantially lowered the fit quality for other lightcurves were also discarded. The lightcurves older than around 1980 had to be discarded because their absolute rotational phases could not be calculated precisely enough due to the period uncertainty (see the seventh section for a more detailed explanation of why absolute phases are needed). Fourteen lightcurves have met the above criteria, in addition to the new lightcurve 15; data on these lightcurves are given in Table 6.

Most papers with lightcurves virtually do not contain any information on errors, which, of course, makes any analysis of those lightcurves more difficult and uncertain. For such lightcurves, uncertainties were estimated by comparison with other papers that provided the uncertainty data and contained observations of objects with similar brightness using similar instruments. These estimations are, of course, only approximate and are not statistically well defined; unfortunately, this was the only way to take into account the uncertainties of those lightcurves.

Table 6. References and observational geometries for lightcurves used in the modelling procedure.

No.	Reference	λ (°)	β (°)	α (°)	Δ (AU)	r (AU)
1	Schroll, Schober, Lagerkvist 1981.	106.6	–16.7	1.4	2.235	14.4
2	Birch, Taylor 1989.	56.7	–17.1	19.4	1.147	2.004
3	Birch, Taylor 1989.	252.8	18.5	6.6	2.326	3.291
4	Birch, Taylor 1989.	186.2	4.7	2.4	1.962	2.953
5	Birch, Taylor 1989.	183.6	5.3	2.4	1.978	2.971
6	Birch, Taylor 1989.	180.5	5.9	7.3	2.050	3.001
7	Birch, Taylor 1989.	179.3	6.1	9.7	2.105	3.016
8	Di Martino, Zappala, De Sanctis, Cocciatoni 1987.	30.2	–16.5	8.0	1.051	2.024
9	Dotto *et al*. 1995.	157.7	–8.2	10.6	1.571	2.487
10	Hainaut-Rouelle, Hainaut, Detal 1995.	287.4	14.5	13.2	1.980	2.834
11	Harris *et al*. 1989.	110.0	–15.2	29.6	1.729	2.021
12	Harris *et al*. 1989..	117.7	17.9	26.6	1.482	2.057
13	Harris *et al*. 1989.	119.0	–20.2	19.4	1.294	2.103
14	Harris *et al* 1989.	107.9	–11.2	23.0	1.730	2.323
15	This paper	323.9	11.6	8.8	1.679	2.642

Lightcurves 8, 10 and 11-15 also provide uncertainties; for the other lightcurves, uncertainties were estimated as described. All the lightcurves were in V band (although different authors define it slightly differently), except lightcurve 15 which was observed in R band, as mentioned in the previous section. This lightcurve was reduced to the V band (550 nm) using the V-R (550 nm and 660 nm, respectively) given in Schober, Schroll 1982. This enabled the investigation of the effects of using lightcurves from different bands, which is often done in practice (although most authors do not stress it explicitly) since the spectral range of the "V band" varies as much as 60 nm among different authors (e.g. Schober, School 1982; Harris 1989; Martinez, Klotz 1998). It will be shown that it is generally true that the systematic errors induced in this way are overruled by the increase of precision and stability due to more data. Details about this will be presented in the following sections.

4. Fourier Expansion of Lightcurves and Period Determination

Fourier expansion of lightcurves is a well-studied topic; many numerical techniques for this task have been developed thus far. The most suitable way for the Fourier analysis of a large number of lightcurves, seems to be the one based on the statistical inversion method, developed by Karttunen and Muinonen (1990). Their procedure is slightly generalised here so that all the lightcurves could be fit simultaneously. The mathematical formalism of this method can be found in the mentioned reference (Karttunen, Muinonen 1990); only the intrinsic properties of this procedure will be presented here.

Each lightcurve was first interpolated so that all the lightcurves contain the same number of points (that is why sparse or unequally distributed lightcurves could not be used). The lightcurves were then expanded as a complex-valued Fourier series (complex form is more suitable for the calculations; the real-valued parameters are to be obtained later):

$$L_m(t) = \sum_{n=1}^{N} C_{mn} \exp \frac{2n\pi_i}{P} t,\ m = 1,\ \ldots\ M \qquad (1)$$

where L_m denotes the m-th lightcurve, c_{mn} is the n-th coefficient of that lightcurve, while P denotes the value for the period (P_o = 0.3004 d, from the Uppsala Spin Vectors Catalogue of Asteroids was the first guess). Let M denote the number of lightcurves, and L and l the number of points per lightcurve and the l-th point, respectively. In order to determine the optimal number of harmonics used, the whole fitting procedure was repeated

with an increasing number of harmonics and the F-test (which gives the probability that the new fit gives more information) was performed:

$$F = \frac{\frac{\chi'^2 - \chi^2}{\nu'^2 - \nu^2}}{\frac{\chi'^2}{\nu'^2}} \tag{2}$$

where χ^2, χ'^2 denote the chi-square statistic and ν, ν' the number of degrees of freedom for the old and for the new fit, respectively. Following Karttunen and Muinonen, the measured brightness' are denoted by **I**, and the desired real-valued Fourier coefficients by **w** (**I** and **w** now being matrices instead of vectors, as a consequence of gathering all the lightcurves together). Three-dimensional covariance matrix is denoted by **S**, and the so-called Fisher information matrix (also three-dimensional) by **Q**.

Since the period is a non-linear parameter, and the Fourier coefficients are linear parameters, there is no practical procedure for solving these parameters without either linearisation of the model or performing small variations of the period to find the best fit. The linearised model proposed by Karttunen and Muinonen is not applicable when fitting many lightcurves simultaneously, so the whole procedure was iteratively repeated by starting from the initial guess and then solving it for parameters, again using a slightly increased and slightly decreased period; the value which gives the better fit was then accepted, and the whole procedure was repeated. The Fourier coefficients were determined so that they maximise the a posteriori probability of the solution, assuming

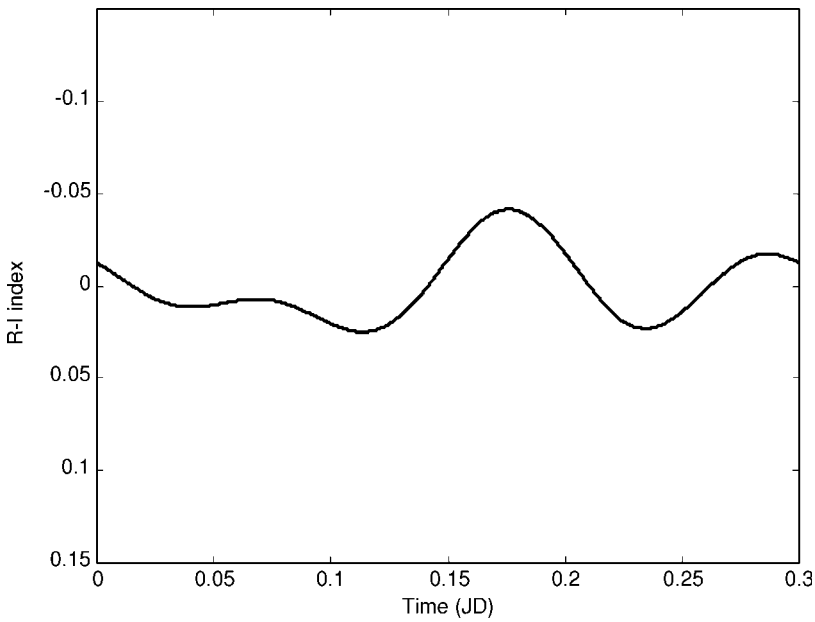

Figure 3.
The curve of $R-I$ index from lightcurves 15. The error of the index in magnitudes is 0.06.

Slika 3.
Kriva *R–I* indeksa krivih 15. Greška indeksa u magnitudama je 0.06.

both the a priori distribution and the a posteriori distribution to be Gaussian. The final equation for the real-valued parameters is:

$$\mathbf{w} = (\mathbf{Q}^{-1}\mathbf{f}^{\mathrm{T}}\mathbf{S}^{-1}\mathbf{I})^{\mathrm{T}} \tag{3}$$

where $\mathbf{Q}$ denotes the Fisher information matrix, and $\boldsymbol{f}$ is an $L\times 2N\times M$ matrix given by:

$$f_{\min} = \cos\left(\frac{2n\pi}{P}\, t_{ml}\right),\ n = 1,\ \ldots,\ N \tag{4}$$

$$f_{\min} = \sin\left(\frac{2n\pi}{P}\, t_{ml}\right),\ n = \mathrm{N} + 1,\ \ldots,\ 2N \tag{5}$$

The described method allows one to obtain the Fourier expansion and period of lightcurves, providing smoothness and stability of the solution. It is important to notice that a self-consistent value of the period cannot be determined if single lightcurves are fit because the period is intrinsically unique for all the lightcurves. The most dangerous part of the simultaneous fitting is the interpolation, which can, in principle, induce large systematic errors; this can be avoided by using only sufficiently dense and equally distributed lightcurves. These lightcurves tend to have a similar number of points, as can be seen from the Uppsala catalogue (and which was the case for the lightcurves used in this paper), so the errors are reasonably small and the overall precision is not much affected.

A Fourier analysis of longer periods was also performed to investigate possible precession, since some asteroids are known to have a non-principal state of rotation (e.g. Simonenko 1985; Harris 1987). However, accurate analysis of these effects requires the time span between any two lightcurves to be much smaller than it was in this case; the results should only be considered as indications.

5. Qualitative Analysis of Lightcurves

Although it is not a widespread practice to pay much attention to qualitative discussion of the lightcurves, it is obvious that some interesting conclusions can be drawn, especially about topics such as albedo variegation that usually cannot be determined in a quantitative way. Some conclusions of this kind have proven to be helpful during the photomorphographic modelling procedure.

Coarse inspection of the lightcurves shows typical properties of a rotating ellipsoid, with two maxima and two minima which are clearly visible. However, the secondary extremes greatly vary depending on the observational geometry, and sometimes even nearly vanish (e.g. lightcurve 4). The amplitude and other properties also differ in different apparitions more than it is usual;

e.g. lightcurves 8 and 9 have quite different properties. In principle, such a strong dependence on the observational geometry encourages the statement that the main reason for the light variations is the shape, and not the albedo variegations. This conclusion is in clear disagreement with some earlier researches (Schroll et al. 1982; Harris 1987). However, it must be stressed that those researches were based only on a qualitative analysis, without giving any quantitative models of Juno; the number of lightcurves used was also significantly smaller. Therefore, the above statement is probably more reliable (photomorphographic modelling has confirmed these conclusions). However, the Fourier coefficients show a significant first harmonic, in some lightcurves (5, 15) even more significant than the second one. The first harmonic is generally thought (and it is quite obvious) to appear due to albedo variegations, rather than shape, although, to be precise, it can also be induced by irregular, non-ellipsoidal shape, and the above statement is true only if some a priori assumptions of the shape are introduced; in general, there is no way to distinguish these effects (Russell 1906; Kaasalainen et al. 1992). It will be shown (section 8) that the first harmonics probably originate from a combination of both mentioned factors, which can be the reason for their intensity. The higher order harmonics are mostly insignificant.

Another interesting possibility is to compare the lightcurve 15 in R and I band. It has often been suggested (e.g. Lagerros 1996; Magnusson 1991; Magnusson *et al*. 1997) that phase difference between lightcurves in different bands is an indication of the surface inhomogeneties. Variations of the colour index curve also indicate such inhomogenities. However, it is very important to understand that the following conclusions are very speculative, based on only one lightcurve, and therefore should be treated with great caution. For a more complete analysis, one should refer to the seventh and eighth section.

The curve of *R–I* index is given in Figure 3. The mean value of the index $R-I$ is found to be: $R - I = 0.56 \pm 0.06$

According to the Uppsala Photometric Catalogue, this is the first published R-I index of Juno. The peak of the colour index can be seen approximately between the second minimum and the second maximum. It should be understood that, as it is usualy the case, the error of the index is quite large, so all the other deviations from the mean value in Figure 3 are within the error range and therefore cannot be discussed. On the mentioned peak, the brightness in I band drops significantly. According to the standard thermal model of asteroids (Lebofsky, Spencer 1989; according to: Lagerros 1996), such features indicate inhomogenities of thermal conductivity in that area of the surface. Namely, in the less conductive area, the surface absorbs a larger amount of thermal energy and thus emits thermal radiation, so the overall flux is the sum of reflected and emitted en-

ergy, and that area also radiates while in shadow. On the other hand, due to the low thermal conductivity of the asteroid, the area which is currently in shadow does not get energy at all (because practically no heat can be conducted from the daylight side), so the emission from the night side is reduced (practically equal to zero). Some curves of colour indices have been successfully explained in this way (e.g. Magnusson *et al*. 1996, Magnusson *et al*. 1997). However, this is a more speculative conclusion, since the I band is the limit between the visual and the infrared light. Although Lebofsky and Spencer, as well as Lagerros (in papers about his new thermal model: Lagerros, 1996, 1997), state that these conclusions are true, at least theoretically, also for the "very near infrared", one should be careful with the above stated consideration. Many more observations, in many more spectral bands, are necessary to confirm it.

Most lightcurves show the difference between the primary and secondary maximum. Although usually also referred to albedo variegations and similar surface inhomogenities (Barucci *et al*. 1992; Dotto *et al*. 1995; Magnusson *et al*. 1997; Schroll, Schober, Lagerkvist 1981; Schober, Schroll 1982), this is largely a consequence of inferior modelling techniques, failing to describe the shape properly, and thus requiring "Harlequin-patched" surfaces. Similar to the discussion of the first harmonic coefficient, there is also no way to distinguish shape and albedo effects from the presented observations. The analysis of the Laplace coefficients (seventh and eighth section) will help to draw more certain conclusions about this.

6. The AAS Method

Modelling the shape and surface characteristics of an asteroid from lightcurves is still an open problem. Some assumptions and approximations are always needed. Classical methods use the ellipsoidal model, which is, among such simple models, probably the most suitable one, especially for large asteroids (e.g. Muinonen, Lagerros 1998; Simonenko 1985). Having more sophisticated methods to use (Barucci, Fulchignoni 1988; according to: Barucci *et al*. 1992; Ostro, Conelly 1984; according to: Kaasalainen *et al*. 1992), the reasons for applying classical methods fade. However, since they do not require many lightcurves or extensive numerical calculations, they are still quite useful. In this paper, the ellipsoidal model is used for a different purpose: to be used as the first guess for photomorphography. The primary role of the classical model in this paper is to give the pole solution which is to be used in photomorphography. Unlike the standard procedure (Kaasalainen *et al*. 1992) which starts modelling from the sphere, the modelling in this paper started from an ellipsoid, thus also using the ellipsoidal shape solution, which has proven to yield a more stable and smooth solution with finer details (see the eighth section).

Classical methods can be classified into two well-known classes: the epoch method (E method) and the amplitude-magnitude method (AM method). Both methods require some assumptions about the lightcurve properties (E method) or the shape and scattering properties of asteroids (AM method). In this paper the method named AAS method is used. It combines the amplitude-aspect relations (Pospieszalska-Surdej, Surdej 1985; Magnusson 1986) and the extraction of spherical harmonics (Lumme *et al*. 1989). It is important to state that the main purpose of this method was not to produce particularly fine axial ratios, but rather to get the coordinates of the pole. However, it turns out that the shape solution is also in reasonable agreement with the results published thus far (see the eighth section). Therefore this method can also be recommended if only the ellipsoidal solution is needed.

The basic idea of the AA part is the use of an aspect-amplitude relation (Magnusson 1986), corrected so that it contains the amplitude dependence from the phase angle in the analytical form, rather than using the amplitudes reduced (to the zero phase angle) by means of linear corrections. The mathematical formalism is based on the results of Pospieszalska-Surdej and Surdej (1985).

In the AA (aspect-amplitude) part of this method, the asteroid is assumed to be a triaxial ellipsoid with the semiaxes $a > b \geq c$ and the pole ecliptic coordinates λ_o, β_o, the c semiaxe being the rotation axis. Let ϑ be the aspect angle, λ and β the ecliptic coordinates of the asteroid, α the phase angle, and ψ the rotation angle (the angle for which the asteroid has rotated measured from the position in which the brightness is maximal). The above notation also applies to the rest of the paper, unless explicitly specified otherwise.

The formalism of Pospieszalska-Surdej and Surdej (1985) will be discussed here in a few words. Based on the well-known Lommel-Seeliger's law (Hapke-Irvine relation), it can directly be concluded that, for the opposition or nearly-opposition observations, the amount of the light received is proportional to the projection of the visible surface of the asteroid ("cross-section"). When all the non-opposition effects (limb darkening, occultation effect, etc.) are neglected, it can be shown that the projection of the observed surface is:

$$S_o(\vartheta, \psi) = abc\pi \left[\sin^2\vartheta \left(\frac{\sin^2\psi}{a^2} + \frac{\cos^2\psi}{b^2} \right) + \frac{\cos^2\vartheta}{c^2} \right] \tag{6}$$

For non-opposition geometry the most significant effect is the occultation effect. The visible cross-section has to be corrected to take into account the nonilluminated part of the visible surface:

$$S(\vartheta,), \alpha, \psi) = S_o(\vartheta, \psi) - \frac{\alpha^2}{4} f(\vartheta, O, \psi) \tag{7}$$

It is clear that equation (6) is a very good approximation for sufficiently small phase angles, but for $\alpha > 17°$ the occultation effect cannot be neglected. The analytical expression for the function $f(\vartheta, O, \psi)$ is too complicated for practical purposes in its most general form (dependence on the aspect angle, obliquity and rotation angle are omitted for the sake of conciseness):

$$f = \pi abc \frac{\dfrac{\sin^2\vartheta\cos^2 O}{a^2b^2} + \dfrac{(\sin\psi\sin O + \cos\psi\cos O\cos\vartheta)^2}{a^2c^2} + \dfrac{(\cos\psi\sin O - \sin\psi\cos O\cos\vartheta)^2}{b^2c^2}}{\left[\sin^2\vartheta\left(\dfrac{\sin^2\psi}{a^2} + \dfrac{\cos^2\psi}{b^2}\right) + \dfrac{\cos^2\vartheta}{c^2}\right]^{\frac{3}{2}}} \tag{8}$$

However, if some reasonable assumptions are made, relatively simple expression for the projection can be obtained. The obliquity can be neglected for most mean-belt asteroids, at least at phase angles less than about 25° (e.g. Tancredi, Gallardo 1990; Kwiatkowski 1995). After some elementary calculations, it can be shown that the values of the function (8) at the lightcurve extrema are:

$$f_{\max}(\vartheta) = (abc\pi)^2 \frac{1}{a^2} \frac{1}{S_{\mathrm{o}\max}(\vartheta)} \tag{9}$$

$$f_{\min}(\vartheta) = (abc\pi)^2 \frac{1}{a^2} \frac{1}{S_{\mathrm{o}\min}(\vartheta)} \tag{10}$$

where $S_{\mathrm{o}\max}$ and $S_{\mathrm{o}\min}$ denote maximal and minimal value of the projection (6), reached for $\psi = 0$ and $\psi = \dfrac{\pi}{2}$, respectively. By supstituting (9-10) into (7) and performing elementary calculations, the dependence of the ratio of the extremal projections from the aspect angle and the phase angle is obtained:

$$\frac{S_{\min}(\vartheta,\alpha)}{S_{\max}(\vartheta,\alpha)} = \left[\frac{1+\cos^2\vartheta\left(\left(\dfrac{a}{c}\right)^2 - 1\right)}{\left(\dfrac{a}{b}\right)^2 + \cos^2\vartheta\left(\left(\dfrac{a}{c}\right)^2 - \left(\dfrac{a}{b}\right)^2\right)}\right]^{\frac{1}{2}} \frac{\left(\dfrac{a}{b}\right)^2 + \cos^2\vartheta\left(\left(\dfrac{a}{c}\right)^2 - \left(\dfrac{a}{b}\right)^2\right) - \dfrac{\alpha^2}{4}}{1+\cos^2\vartheta\left(\left(\dfrac{a}{c}\right)^2 - 1\right) - \dfrac{\alpha^2}{4}\left(\dfrac{a}{b}\right)^2} \tag{11}$$

If the scattering effects are neglected, the amplitude can be expressed again from the expressions for the illuminated visible surface (dependence from the

aspect angle and phase angle is not included for the same reason as in (8)):

$$A = 1.25\log\frac{1+\cos^2\vartheta\left(\left(\frac{a}{c}\right)^2-1\right)}{\left(\frac{a}{b}\right)^2+\cos^2\vartheta\left(\left(\frac{a}{c}\right)^2-\left(\frac{a}{b}\right)^2\right)}+2.5\log\frac{\left(\frac{a}{b}\right)^2+\cos^2\vartheta\left(\left(\frac{a}{c}\right)^2-\left(\frac{a}{b}\right)^2\right)-\frac{\alpha^2}{4}}{1+\cos^2\vartheta\left(\left(\frac{a}{c}\right)^2-1\right)-\frac{\alpha^2}{4}\left(\frac{a}{b}\right)^2} \qquad (12)$$

As it can easily be seen, the above equation becomes the classical Magnusson's aspect-amplitude relation if the phase angle equals zero. Although the above relation is a very simplified model of the actual amplitude dependence from the observing geometry and shape parameters, it can be stated that the amplitude-phase angle dependence is taken into account quite satisfyingly. Numerical experiments were carried out with a few dozen asteroids which had polar orientation and axial ratios among the best determined thus far. These parameters were taken from the Uppsala Catalogue of Spin Vectors of Asteroids. The accordance of the simulated amplitudes with the observed ones (taken from the Uppsala Photometric Catalogue) is good in most cases. No significant difference among different taxonomic types can be noted, although the S type should, theoretically, show the largest inconsistencies with the equation (12) since its surface induces significant multiple scattering effects. This is probably due to relatively small phase angles; as the phase angle increases, the accordance quickly vanishes.

The traditional procedure for interrelating the aspect-amplitude relation with the polar orientation is not convenient in this case, so the well-known relation for the aspect angle was used as an additional equation:

$$\cos\vartheta = -\sin\beta\sin\beta_o - \cos\beta\cos\beta_o\cos(\lambda-\lambda_o) \qquad (13)$$

Therefore, each lightcurve gives one pair of equations (12-13), and the whole set is then solved in β, λ, a/b, a/c space. For this particular case, there were thirty equations with four unknowns. However, it is important to understand that equations (12-13) are separated only for calculational purposes, and that these thirty equations are in fact equivalent to fifteen equations, one for each lightcurve, as it is usual for AA methods. Since equation (13) should be treated as an identity (as it is the case in both Pospieszalska-Surdej, Surdej 1985 and Magnusson 1986), the numerical procedure performed to find the solution should also treat it as a constraint which has to be identically satisfied for any observational geometry. Some advanced equation-solving algorithm should be used here (a somewhat modified sequential quadratic programming algorithm was used in this paper). The amplitudes

we-re obtained from the Fourier coefficients calculated in the previous section. This approach is more reliable and simpler than the use of differences between the minimal and maximal brightness. The obtained pole solution was used as the starting guess for the S part of the whole procedure.

The spherical harmonics part of the method is not model dependent and it does not use any shape parameters as a starting guess nor does it give any shape parameters as a result. This feature makes it less vulnerable to systematic errors than the classical procedures. This part is essential for a precise determination of the pole, which is needed for the photomorphography. The only practical limitation is that good a priori knowledge of the pole position is required: the results of the AA part are used at this point. The method is based on amplitudes and magnitudes, but includes a quite different approach and mathematical formalism than the classical amplitude-magnitude techniques. The method is described in Lumme, Karttunen, Bowell 1989. Originally, it uses only the second order amplitude term in the spherical harmonics expansion, which has to be reduced to the zero phase angle. In order to avoid as many potential sources of systematic errors as possible, in this paper a slightly different version which does not require any reduction of amplitudes was applied.

The mathematical formalism of this procedure is based on Laplace series (or spherical harmonics series) expansion. The expansion of the brightness with respect to the aspect angle and the rotation angle can be written in the following form (the usual normalising coefficients are omitted, as they are not necessary here):

$$L(\vartheta, \psi) = \sum_{l=0}^{L} \sum_{k=0}^{l} b_{lm} P_l^m (\cos\vartheta)\, e^{im\psi} \tag{14}$$

where the Legendre polynomials are denoted as usual, and b_{lm} are the coefficients carrying the information on the lightcurves. The power spectrum of the previous equation is more convenient for practical purposes:

$$H(\vartheta) = \sum_{l=m}^{L} h_{mj} P_l^m (\cos\vartheta) \tag{15}$$

Unlike the original procedure (Lumme *et al*. 1989), two amplitude terms were used (H_1, H_2); this should make the solutions more reliable, particularly because, as it was mentioned in the previous section, some lightcurves contain significant odd harmonics (in fact, first order harmonics; the higher order harmonics are mostly negligible). Reduction of the amplitude terms was avoided by introducing terms h'_m characterising the phase angle influence, thus making the above terms directly dependent on

the phase angle; analytical expressions for this influence and their derivation are not important here and will be published elsewhere. Aspect angle was substituted from the equation (13), thus making the above equations dependent from the desired polar orientation.

Due to the large number of lightcurves available, an expansion to the fourth order could be performed:

$$H_1 = \sum_{l=1}^{4} h_{1l}\, h'_1\, P_l^1\,(cos\vartheta) \tag{16}$$

$$H_2 = \sum_{l=2}^{4} h_{2l}\, h_2'\, P_l^1\,(cos\vartheta) \tag{17}$$

If there are K lightcurves, 2K equations are obtained (one for each aspect angle), containing altogether 2L+1 unknowns; so, using fifteen lightcurves, there were thirty equations containing nine unknowns. For this set the same statement as for the set (12-13) applies: it requires a good solving algorithm, especially because the first order coefficients, although not negligible, are generally smaller than the second order coefficients; dependence on the phase angle also induces some instability. It is now clear why a good first guess for the pole was needed: only minor changes of the aspect are made during the solving procedure in this case, thus making the fit "nearly linear", since the most extensive calculations are done when solving for the expansion coefficients h_{ml}. The Levenberg-Marquardt minimisation routine was used in this paper, and it has proved to be more convenient than the programming methods for this case.

7. Photomorphographic Shape Analysis

Photomorphographic analysis is probably the best modelling technique currently available (see the ninth section for a more detailed discussion). It is rather demanding because it requires a very good solution for the spin vector, and the calculation of the shape parameters is a very tricky numerical procedure which requires the use of regularisation methods and inversion. However, as it will be shown, the results are rather interesting and informative.

This method was developed by Kaasalainen and his collaborators (Kaasalainen *et al*. 1992). In this paper a procedure similar to their original method is used, except some minor changes and an entirely different numerical method used for solving the shape. The basic idea of the photomorphographic method is to make the dependence of the lightcurves from the shape properties more general; the shape parameters are therefore obtained by inverting the integral brightness equation. No "global" assump-

tions on the shape are needed, except the convexity; also, there is no predefined shape, such as an ellipsoid.

The mathematical formalism of photomorphography will now be described in a few words. Two coordinate systems will be used: the first being the Earth-Sun based system, which parameterises each point on the surface with four angles introduced earlier: aspect angle ϑ, obliquity O, phase angle α and absolute rotation phase ψ (note that ψ is not the rotation angle used in the previous section), while the second coordinate system is the intrinsic feature of this method. This system parameterises a point with the direction (in spherical polar coordinates θ, φ corresponding to "longitude" and "co-latitude", respectively) of an outward unit which is normal at that point. This is the well-known "Gaussian mapping". It can be easily shown that this mapping describes a unique shape if and only if it is strictly convex (convex without planar sections). This is the most severe limitation of this method, although some concavities can be added subsequently, as it will be shown later.

The integral brightness can be expressed as:

$$L(\theta,\varphi;\,\vartheta,O,\alpha,\psi;\,P(\iota,\varepsilon,\alpha,\mathbf{Q})) = \iint_S P(\iota,\varepsilon,\alpha,\mathbf{Q})\, G\,(\theta,\varphi)\,\sin\varphi\,\mathrm{d}\theta\,\mathrm{d}\varphi \quad (19)$$

where $P(\iota,\varepsilon,\alpha,\boldsymbol{Q})$ denotes the scattering law ($\boldsymbol{Q}$ being the vector of physical parameters in the scattering law), and $G(\theta, \varphi)$ is the Gaussian surface density, one of the standard concepts of differential geometry; its meaning is easily understood knowing that:

$$\mathrm{d}S\,(\theta, \varphi) = G\,(\theta, \varphi\upsilon)\,\sin\varphi \quad (20)$$

Explicit knowledge of the surface density defines the shape, thus being the solution of the problem. Integration area S corresponds, of course, to the visible and illuminated part of the surface; these conditions can be easily parameterised using, for example, the angles ι, ε and the relations that connect them with the Gaussian coordinates θ, φ.

Equation (19) is a Fredholm equation of the first kind, famous for its ill-conditioned nature; the Gaussian mapping is the only one among the well-known coordinate systems which allows the integration limits to remain constant; unfortunately, this makes the inversion itself very tricky. Following Kaasalainen (Kaasalainen, Lamberg, Lumme, Bowell 1992), the equation was solved in the form of Laplace coefficients of a spherical harmonics expansion:

$$G\,(\theta, \varphi) = \sum_{l=1}^{L} \sum_{m=-l}^{l} b_{lm} Y_l^m\,(\theta, \varphi) \quad (21)$$

b_{lm} being the unknown coefficients. On the other hand, the lightcurves are known in the form of Fourier expansion (1). If the mentioned expansion is rescaled and reshaped so that it gives brightness as a function of the absolute rotational phase:

$$L(\psi) = \sum_{n=-\frac{N}{2}}^{\frac{N}{2}} c_n \exp(in\psi) \tag{22}$$

it can be equalled with equation (21). Of course, the latter equation first has to be transformed so that it becomes explicitly dependent only on the absolute rotational phase. Since this transformation is completely identical to that described in Kaasalainen *et al*.1992, there is no reason for repeating their formalism here; it is enough to say that the final form of the equation (21) is:

$$L(\psi) = \sum_{l=0}^{L} \sum_{m=-l}^{l} b_{lm} k_{lm} \exp(im\psi) \tag{23}$$

The coefficients denote all the transformation terms collected together. By equalling (22) and (23) one obtains:

$$c_m = \sum_{l=\mathrm{đ}m\mathrm{đ}}^{L} b_{lm} k_{lm} \tag{24}$$

A set of equations for b_{lm} is thus obtained, depending on lightcurves (the coefficients c_{m}), observational geometries and scattering properties of the surface (the latter two being characterised by k_{lm} coefficients). The above set of equations was solved with one of the inversion techniques (maximum entropy method). Details of the calculations are given in section seven. There are several reasons for the inconvinience of the above equations. First, it is clear that the request for all the Gaussian mapping coefficients to be non-negative and sufficiently small if they are of a high degree (because the series has to be convergent) poses non-standard constraints, which require advanced numerical techniques. Small uncertainties may induce large deviations among the final solutions.

The scattering law is contained in k_{lm} coefficients. It is immediately clear that it has to be of a suitable form so that none of these coefficients vanish, in which case some data describing the shape would be lost. Since the actual scattering properties of the surface are probably complex in comparison to any theoretical scattering law, there is no risk that such loss of information actually happens in the lightcurves but it may happen in equations (24) because of the use if an inconvenient scattering law. Fortunately, as it has been shown (Kaasalainen *et al*. 1992), with non-opposition ob-

servational geometry, simple laws, such as the combination of Lambert law and Lommel-Seeliger law, are applicable; the Lumme-Bowell law is also convenient. Therefore, the Lumme-Bowell law was used to describe the scattering since it is rather general and allows some coarse description of physical properties of the surface; parameters for S type asteroids (Karttunen, Bowell 1989) were used. The scattering parameters can be deduced easily, since the equation (24) then becomes:

$$c_m = \sum_{l=|m|}^{L} b_{lm} \sum_i k_{lmi} \tag{24}$$

where k_{lmi} are the terms which contain parameters of the scattering law in the form of a sum of expressions depending on the incidence and emittence angles, phase angle and location. In practice, it has turned out to be impossible to take into account dependence of albedo from the location if the scattering coefficients are also taken as unknowns because the lightcurve number was not large enough. In order to investigate the albedo map, a "blend" of Lambert and Minnaert law (the latter is given in e.g. Barucci *et al*. 1992) was constructed:

$$P(\iota, \varepsilon) = (\cos \varepsilon)^{2\mu - 1} (cos\, \iota)^{2\nu - 1} \tag{26}$$

where μ, ν denote non-dimensional coefficients, the former of order unity and the latter somewhat smaller: these values have given the most realistic synthetic lightcurves in numerical experiments (lightcurves can easily be simulated using equation (19), since the Gaussian surface density, the scattering law and the observational geometry are in that case explicitly known). Although very simple and apparently without much physical sense, this law was convenient for calculating albedo variegations because it includes only two parameters with best values that can easily be found by performing small variations. The coefficients k_{lm} in equations (24) can be multiplied by the location dependent albedo function; however, the number of lightcurves has again proven to be of crucial importance. For determination of the more sensible physical parameters of the surface, the Lumme-Bowell law was used again, in the form given in Karttunen 1989.

The second interesting point is the refinement of the spin vector solution. As it was pointed out by Kaasalainen and his collaborators, small errors in the spin vector do not affect the solution very much, but the period has to be known very accurately (because absolute rotational phases are used). Simultaneous solution of all these parameters is difficult in practice because the equation (19) is linearly dependent on the shape but nonlinearly dependent on the spin vector. The simplest approach would be to use small variations to obtain the best fit (similarly as in the fourth section). This approach was also used in our calculations.

Finally, there is the problem of calculating the surface points (precisely, their radius vectors) from the Gaussian surface density. This task is not as numerically complicated as the calculation of the Gaussian mapping itself because there are no problems with instability; as it was shown (Minkowski 1903) the Gaussian mapping uniquely determines the surface, not only by means of radius vectors, but also by means of the support function (outer product of an outward surface normal and the corresponding radius vector). The support function is convinient for the radius vector determination, since the direct relations between the surface density and the radius vectors lead to a complicated set of coupled second-order non-linear partial differential equations. The support function was calculated using the concept of the so-called mixed volume, introduced by Minkowski (Minkowski 1903) and proposed in the mentioned Kaasalainen's paper (Kaasalainen *et al*. 1992). This concept is well-known (e.g. Nurenberg 1953, according to: Kaasalainen *et al*. 1992; Mecke 2000) so there is no need to describe it here in great detail. The minimisation algorithm used to solve the support function is the iterative technique mentioned in Mecke 2000. Knowing this function, elementary use of differential geometry gives the radius vectors.

8. Results and conclusions

This paper is somewhat illustrative in nature: models of single asteroids are not of significant importance, but if suitable modelling techniques are developed soon, this can help to build a large database of models which can be of use for studies of common properties within the same taxonomic type or within the same orbital family, interrelating shapes with the orbital and collisional evolution, etc. The following results should therefore show the vastness of data that can potentially be obtained from lightcurves.

Fourier analysis described in the fourth section allowed all the lightcurves to be parameterised by means of Fourier coefficients, which are not only more reliable, but also easier to use than discrete points. The best value for the period of Juno (in days) was calculated:

$$P = (0.30040 \pm 0.00001)\ \mathrm{d} \tag{27}$$

The main properties of the lightcurve coefficients are described in the fifth section, more as an illustration of a purely qualitative reasoning (which was common in modelling of asteroids until relatively recently) which can be compared with exact results obtained later, than for any real information, although some preliminary conclusions proved to be helpful while choosing the photomorphographical procedure. Therefore, there is no reason to repeat those conclusions here. It is more interesting to discuss the long-period variations. Although very tentative and speculative, the obtained results do show some quasi-periodical variations of the order of a few days. Spectral power of these variations is barely significant, but it still seems probable that they

are not an effect of noise. Of course, no statements such as the precession of Juno can be made; the noted variations should be treated as small irregularities which can only be prescribed to the existence of forced precession in the distant past (compare similar results and discussion in Krugly *et al*. 1994; Bronsteyn 1982). Little can be concluded from this; it is only obvious that traces of collisional and/or tidal evolution stay detectable long after the direct effects disappear; however, it must be noted again that this result is suspicious.

The AAS method allows calculation of rather stable solutions for the axial ratios and pole orientation. Different combinations of lightcurves were investigated: up to seven lightcurves were discarded, increasing the requests for the percentage covered, goodness of fit, etc. Those lightcurves which were spectrally different from Johnson's V standard (the R band lightcurve (lightcurve 15), and some other lightcurves for which it was found in the corresponding papers that the used filters were not standard) were also excluded from some test calculations. Finally, it was obvious that the quality of the solution becomes better if more lightcurves are added; the given solutions are thus the solutions found when all the lightcurves are taken into account. Details on these questions can be found in the next section.

During the AA step, two solutions were obtained, where the second one obviously gives an unrealistic, extremely flattened shape:

$$\begin{array}{ll} \lambda_{o1} = 105°\pm8° & \lambda_{o2} = 322°\pm8° \\ \beta_{o1} = 39°\pm11° & \beta_{o2} = 57°\pm11° \\ \left(\frac{a}{b}\right)_1 = 1.24\pm0.06 & \left(\frac{a}{b}\right)_2 = 1.56\pm0.06 \\ \left(\frac{a}{c}\right)_1 = 1.43\pm0.10 & \left(\frac{a}{c}\right)_2 = 1.90\pm0.10 \end{array} \qquad (28)$$

The errors given are maximal deviations, not the formal errors, since the latter have unrealistically small values (similar difficulties are often in this kind of problem, e.g. Kwiatkowski 1995; Magnusson *et al*. 1997; see also a more general discussion in Press, Teukolsky, Vetterling, Flannery 1997). The second solution was discarded for both formal and physical reasons: its convergence is very slow, formal errors are an order of magnitude smaller than for the first solution (this being an evidence of the unphysical nature of the solution), the shape is too flattened for a large asteroid such as Juno. Most importantly, the spherical harmonics part clearly showed the unacceptability of this solution; even the spherical harmonics expansion becomes nearly impossible with these starting values. The final result of the AAS method is:

$$\lambda_{o1} = 104°\pm6°$$

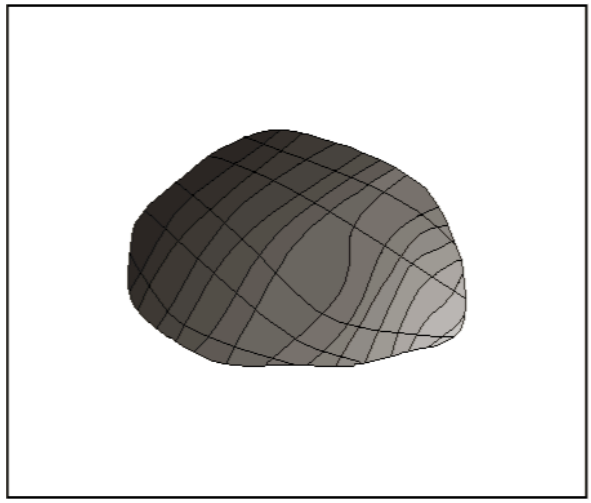

Figure 4.
Model of Juno "seen" perpendicularly to the ab plane – view "from the top"

Slika 4.
Model Juna "viđen" normalno na ravan ab – pogled "odozgo"

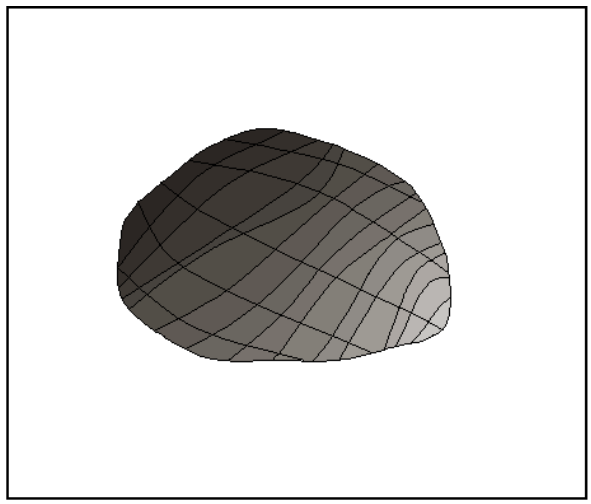

Figure 5.
Model of Juno "seen" perpendicularly to the ab plane – view "from the bottom"

Slika 5.
Model Juna "viđen" normalno na ravan ab – pogled "odozdo"

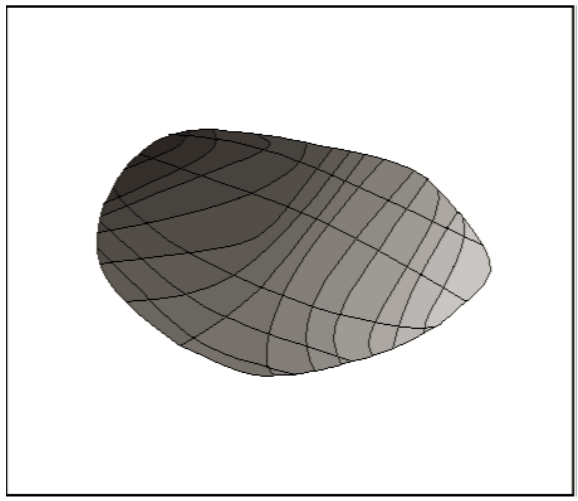

Figure 6.
Model of Juno "seen" perpendicularly to the ac plane – view "from the right"

Slika 6.
Model Juna "viđen" normalno na ravan ac – pogled "sa desne strane"

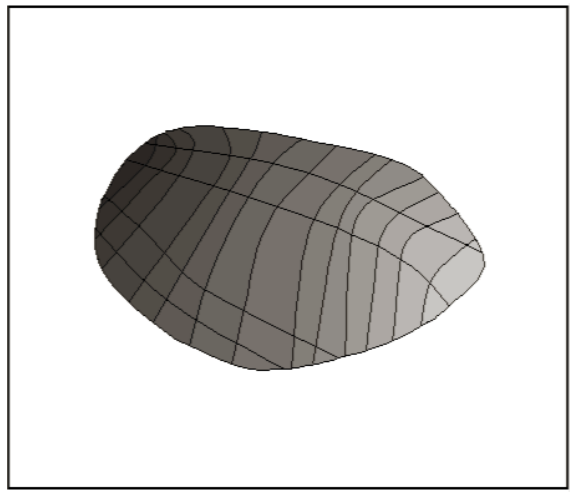

Figure 7.
Model of Juno “seen” perpendicularly to the ac plane – view “from the left”

Slika 7.
Model Juna “viđen” normalno na ravan ac - pogled “sa leve strane”

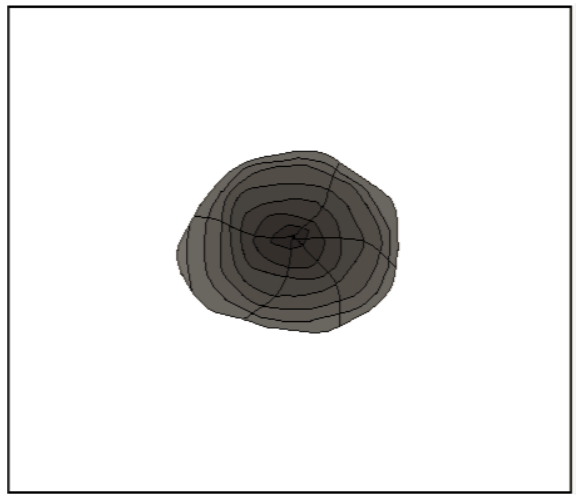

Figure 8.
Model of Juno “seen” perpendicularly to the bc plane – view “from the right side of the previous figures”

Slika 8.
Model Juna "viđen" normalno na ravan bc – pogled “sa desne strane prethodnih slika”

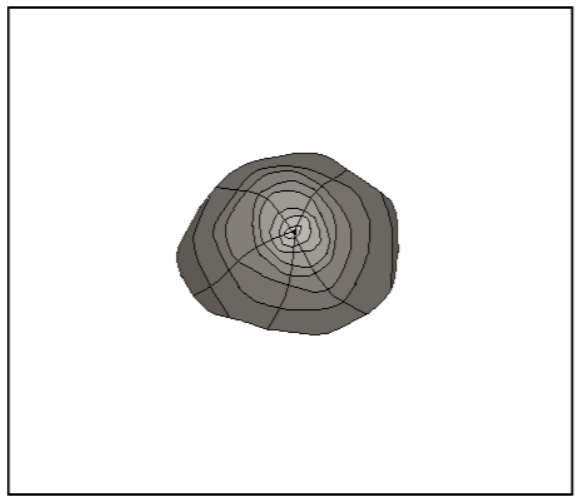

Figure 9.
Model of Juno “seen” perpendicularly to the bc plane – view “from the left side of the previous figures”

Slika 9.
Model Juna “viđen” normalno na ravan bc – pogled “sa leve strane prethodnih slika”

$$\beta_{o1} = 37° \pm 7° \tag{29}$$

The photomorphographical analysis is, of course, the source of most complete and most indicative information in this paper. Many slightly different approaches were tried in order to investigate different properties. The number of lightcurves used was also varied; the results are qualitatively similar to those of the AAS method (best results with the largest number of lightcurves), but propagation of systematic errors is now even more difficult to trace. Polar orientation and period were refined during the modelling, as the maximum entropy method allows simultaneous calculation of linear and nonlinear parameters. The new values, being the final spin vector solution, are:

$$\begin{aligned} \lambda_{o1} &= 104° \pm 6° \\ \beta_{o1} &= 37° \pm 7° \\ P &= (0.30040 \pm 0.00001)\ \mathrm{d} \end{aligned} \tag{30}$$

This is very near to the solution (29); formally, one cannot state that (30) is any better, but bearing in mind the properties of the maximum entropy method, solution (30) was accepted as the best one.

The shape was obtained using both the shape-only equations (24) and the combined shape-albedo equations (25), the latter one with the Lumme-Bowell law and with the law given in (26). Apparently, such an approach is very coarse since it does not allow explicit determination of relative shape and albedo contributions. However, this is common in photomorphography (e.g. Barucci *et al*. 1992). The set of equations (24) gives the shape-only solution, which is also the smoothest and the most rapidly convergent one; therefore, it was accepted as the most probable solution and it is given in Figures 4-9, from six different views (see captions for the corresponding pictures). The light source is arbitrarily positioned and it does not represent any particular observational geometry. The shape contains some concavities, to represent the true shape as well as possible.

The albedo map, obtained from the equations (25) using the scattering law (27), tends to be unstable in the numerical sense and suspicious in the physical sense. The scattering law was constructed to be convenient for separating shape and albedo parts of the Laplace coefficients. Although it does have some physical meaning in very much the same sense as the Minnaert law, corrected for the effects of the angle of incidence so that the surface need not be assumed to be smooth, it remains only a rough approximation. The best values for μ,ν were calculated to be 0.68 and 0.53; the value for μ is in good agreement with the accepted values for S type asteroids in Minnaert law (0.55-0.70 as stated by French, Veverka 1983; according to: Barucci *et al*. 1992), while ν, practically, confirms the con-

venience of the Minnaert law, since the dependence upon the incidence angle is rather insignificant. Of course, the determination of these parameters is also tentative since they are coupled with surface inhomogenities. They are, however, not very significant: the maximal deviation from the mean albedo is about 20%, while two thirds of the surface have variegations not larger than 8%, being probably within the error range.

The global shape, in the case of the albedo-shape model, is similar to the shape-only solution in Figures 4-9, so the main results of albedo mapping may be described using these figures. There are two apparent, significant patches on the surface: one on the mountainous structure, visible near the centre in Figure 4, and one in the lower central region in Figure 6. The second one is in a slightly concave region, best visible in the left centre of Figure 5. Both are darker than the rest of the asteroid.

Finally, modelling was performed using Lumme-Bowell again, only this time to calculate the scattering parameters. This task is numerically difficult, since the number and quality of lightcurves is not sufficient to allow unambiguous determination. To simplify the approach as much as possible, only three free parameters were used: single scattering albedo ω_o, asymmetry factor g and surface roughness ρ; as usual, the surface was assumed to be saturated with holes, giving $q = 1$. The second parameter assumed to be constant is the volume density, for S asteroids about $D = 0.37$ (Karttunen, Bowell 1989). This parameter appears only in the single scattering function, so it would be practically impossible to determine it; on the other hand, most results obtained thus far (e.g. Magnusson *et al*. 1997; Rowe 1993) show that this parameter does not change much among different asteroids, especially among asteroids of the same taxonomic type. The calculated values of the parameters are:

$$\begin{aligned} \omega_o &= 0.57 \\ g &= -0.10 \\ \rho &= 1.19 \end{aligned} \qquad (31)$$

Unfortunately, there is no way to calculate the errors; uncertainties are probably of the order 0.03, but systematic errors are probably much more significant. The standard values for S type asteroids are $\omega_o = 0.54$, $g = -0.07$, $\rho = 1.19$, thus being similar to the calculated values. However, it is interesting that all the calculated values are "more nongeometric" than the standard ones; albedo is larger, asymmetry is more significant, as well as the roughness, all three contributing to nongeometric scattering, more distinct dependence of magnitude and amplitude upon the phase angle, etc. It is also possible that this is a systematic effect due to the approximations or some unknown dependence upon some features in the lightcurves. The shape itself is even more

similar to the shape-only model than in the previous case (probably because of the same scattering law used) but stability of the solution is somewhat reduced.

Errors of the shape itself are also very difficult to determine; this is an important problem with photomorphography, still unsolved. For the shape-only solution, deviations of the calculated lightcurves from the observed ones are about 2%; for the other two models, these deviations also contain the errors of albedo map/scattering coefficients

Based on the above stated, some general conclusions about the physical properties of Juno can be drawn. Firstly, its pole solution is well determined; results presented are in good agreement with those previously published (results of other authors are cited from Uppsala Spin Vectors Catalogue of Asteroids). The longitude of the pole ranges between 101° and 110°, while the latitude is between 29° and 40°. The pole solution given in this paper is probably the most reliable one, since it includes most lightcurves and uses the most general method – spherical harmonics expansion. Some authors also report a second solution that is relatively near to the second ellipsoidal solution in this paper, which is, however, as mentioned, erroneous since it cannot fit the spherical harmonics expansion. The a/b ratio is within the interval 1.18-1.23; the ellipsoidal model in this paper gives a slightly larger ratio – 1.24, due to reasons discussed in the following section. The other shape parameter is reported by other authors as b/c ratio; the result from this paper corresponds to the value 1.15. There are only two reliable solutions for this value so far: 1.02 and 1.26. Therefore, it can be stated that this ratio is not yet well determined; however, for reasons described in the next section, the value published here might be close to the truth, especially because it agrees quite well with the photomorphographical model. As a large S type asteroid, Juno is expected to be nearly spherical and to have a relatively smooth surface. The ellipsoidal solution and, especially, the photomorphographical model, show, however, a somewhat more flattened and irregular shape; some purely local structures, e.g. slight concavities, mountainous structures, etc. are clearly visible in Figures 4-9, although the smallest irregularities are probably the side effects of Laplace series truncation, random errors, etc, rather than real structures. This, together with the possibility of a precession existing some time ago, indicates tempestuous collisional evolution. In light of this assumption, some of the concavities present in the model, especially those with possible albedo patches, can be interpreted as craters. Of course, this is only a possibility. Whereas, also according to results of recent NEAR landing on Eros, it seems that asteroids, including large ones, are more irregular and collisionally evolved than it is usually assumed. The albedo variegations probably do contribute to the overall lightcurve shape. Although details are

very uncertain, it seems that they have some connection with the supposed collisional evolution (e.g. darker surface on the most significant concave feature). It is interesting that the shape is nearly invariant to the existence of albedo variegations; if we assume that this is not a consequence of erroneous calculations (which might be the case), this indicates that the cause of non-shape lightcurve properties might be some unknown properties of the phase curve. The Lumme-Bowell law parameters seem to contribute to the lightcurve shape more than expected; it also seems that the obtained values of these coefficients are more certain than the albedo map. The classic H-G parameterisation of Juno's phase curve was not carried out in this paper since reduced amplitudes and/or magnitudes where not used; another reason is that the H-G system is very sensitive to minor spectral differences in observational data (Lagerkvist, Magnusson 1990).

It would be interesting to carry out a detailed observational campaign to confirm the existence of precession; also, better coverage of both very small (< 5°) and very large (> 30°) phase angles could reveal interesting details; if the hypothesis of a relatively bright, rough, non-geometrically scattering surface is true, the opposition effect, which is still poorly observationally covered for Juno, should be particularly strong. Nevertheless, new observations will reveal more details. More clever numerical techniques may also allow more certain calculations of some surface characteristics.

9. Discussion

Many different methods and numerical procedures are used in this paper, some of them well-known and well-investigated, while some are newly introduced here, or still rarely used or poorly known. Also, many assumptions and standard simplifications are done in the asteroid modelling, which have to be analysed in order to make the modelling more efficient and the results more certain.

Quality of observational data is, generally speaking, very problematic, which probably causes many of the inconsistencies among different authors, even when very similar methods are used. Generally accepted conventions about the publishing and parameterising of data do not exist. As it was already mentioned, many authors do not even publish errors of their observations. It seems that reliability of the results severely drops because of such problems, although more as a result of the different ways in which different authors deal with them than because of the low-quality of the data itself, if the lightcurves are carefully chosen. For test purposes, the models of Zappala and Knežević (Zappala, Knežević 1984, according to: Birch, Taylor 1989) and the models of Birch and Taylor (1989) were calculated using the lightcurves and the methods originally used by them, but

with a more rigorous scheme for taking into account the influence of instrumental errors and different spectral bands on the final error; this resulted in very similar final results and, it seems, more consistent values of errors. The influence of slightly different spectral bands was checked for each method separately, but the overall conclusion is that one should use as many lightcurves as possible, except in extreme cases when the results are substantially affected by the lightcurve inconsistencies. Of course, the need for standardisation of photometrical systems remains one of the most important observational issues.

The Fourier parameterisation and period determination of the lightcurves was carried out by means of one of the theoretically best developed, but in practice still rarely applied method. It is clear that this method is rather demanding in the sense of quality of data; good a priori knowledge of the period is also needed, especially if the period is obtained by small variations. If single lightcurves are fit, as in the original paper (Karttunen, Lumme, Bowell 1990), the calculations have to be linearised so that the period is directly calculated. On the other hand, Fourier coefficients are very self-consistent, even if no good guesses of the amplitude or some other lightcurve features are available. Simultaneous fit of all the lightcurves has proved to be much more convenient and stable than individual fit of each lightcurve, although the reasons for this are not quite clear. It seems that many single fits affect the overall consistency, especially for those curves which differ significantly from most of the others; also, as mentioned, the period cannot be determined in this case, since its determination must include all the lightcurves. The largest problem here is interpolation, which can induce errors itself. Despite some earlier conclusions (e.g. Lumme, Karttunen, Bowell 1989), it is obvious that the good sides of interpolation justify its use; interpolated lightcurves also allow some manipulations (e.g. FFT) which are not possible otherwise.

The aspect-amplitude part of the AAS method needs especially extensive investigations and tests, since it is used here for the first time. The aspect-amplitude relation itself is a very coarse approximation, but it is theoretically justified, unlike the empirical correction of the amplitude in traditional relation (Magnusson 1986). Its usefulness probably greatly depends on the surface characteristics of a particular asteroid. Detailed tests of this procedure are beyond the scope of this paper, but some interesting points can be discussed. As mentioned in the sixth section, the amplitude-aspect relation was tested for the best-observed asteroids and the agreement is surprisingly well. This might be because the occultation effect remains the most important factor in the range of phase angles usually covered by observations. It might be worth noticing that the disagreement between the numerically simulated lightcurves and the predicted amplitudes was con-

siderably larger, especially for large phase angles and for S type scattering parameters. A good explanation for this still cannot be given. One possibility is that the free path of light inside the surface layer of these asteroids is usually larger than the average surface roughness scale, so a portion of light losses information about its original direction and practically does not show any dependence upon the incidence angle. This is only a hypothesis and further work is needed to confirm it.

The ellipsoidal model shows satisfyingly good agreement with previous data, except for the shortest semiaxe. However, as it was noted, many authors experienced difficulties with its determination; for example, Erikson and Magnusson (Erikson, Magnusson 1993; according to: Uppsala Catalogue of Spin Vectors of Asteroids) have calculated two drastically different solutions, one of them being unphysical. Others have assumed Juno to be a biaxial ellipsoid. These facts indicate that empirical relationships may overlook some important, probably mostly geometrical effects. On the other hand, a somewhat larger a/b ratio in this paper does show that the scattering effects are underestimated.

The spherical harmonics expansion, gives better results if the phase angle dependence is taken into account. Of course, this requires a better numerical technique, because more unknown coefficients are introduced but the results are as general as possible, free of any dependence from the shape. This makes the spin vector, together with its refined value during the photomorphography, the most certain and solid result of this paper. Overall, the AAS method has proven to be a good technique. Although techniques which include direct dependence of the lightcurve upon the surface, shape and observational geometry (e.g. Kwiatkowski 1995) are surely more reliable, and can be easily put together with a spherical harmonics method, they are mostly not necessary for the Main Belt Asteroids, because the observational geometry does not change so fast as in the case of Near Earth Asteroids. Also, the use of epochs should improve the results, but it is very difficult because good epochs are not available for most observations (this paper does not use epochs because very few good ones could be found).

The photomorphographic method is, probably, the most perspective technique in this field. This is the only method, which, in theory, gives the best convex shape (in the least-squares sense). No firm preliminary assumptions have to be made, but an a priori guess is very important. Experiments have shown that a sphere always gives worse solutions than somewhat elongated models, even if their axial ratios significantly differ from the shape of the synthetic object. Laplace coefficients of higher order have to be bracketed inside a narrow interval, but the need for this largely fades if a good first approximation is known. Bodies with craters have been simulated with the similar formalism as in the equation (19), using also some results of Kart-

tunen 1989. A global, convex shape is obtained without difficulties. Larger craters have substantially negative values of the Gaussian surface density, but this can be successfully included in the model, as it was done in this case. Of course, intrinsically non-convex bodies cannot be represented.

Albedo variegations and scattering parameters of the surface can, in principle, be obtained by means of ordinary procedures if there are enough different observational geometries. For this purpose, a few well-distributed lightcurves have proven better than large numbers of lightcurves that cover small intervals of the phase angle. The "combined law" used in this paper gives a coarse description of the albedo distribution; most significant inhomogenities are well modelled, while the others are drowned by noise. It can be said that the conclusion of the albedo variegations of Juno in the previous section is justified (only two regions with lower albedo, the rest is noise). The Lumme-Bowell law with fixed parameters is best for reproducing synthetic curves, while the parameter determination is somewhat problematic: many lightcurves (at least about 15) are needed and extremely irregular shapes produce larger values than the true ones. Although exactly 15 lightcurves were used for Juno and the shape is probably not very irregular, it should be clear that a systematic error for the parameters obtained does exist.

Local concavities can be restored during the calculation of the support function using ideas very similar to those mentioned in the fourth section and used for the Fourier analysis and based on statistical inversion. The intrinsic idea is that in those regions of the surface in which the support function does not give meaningful results, the Gaussian surface density is inverted so that those values which give the best shape and which are satisfyingly near to the starting values are found. This is a mathematically suspicious idea, since the solution is somewhat subjective, but numerical experiments have shown that the shape can be reconstructed satisfyingly with relativley few erroneous structures, induced by subjectivity. Of course, this approach also requires further developments.

Good numerical techniques are very important in this paper. It cannot be stated that the maximum entropy method really is the best choice, but it does have some good characteristics: smoothness, stability, intrinsic non-negative values of the results and non-linearity, which allows the simultaneous determination of the spin vector together with the shape. Of course, the method used here is only formally similar to the traditional maximum entropy image restoration techniques, since it includes a priori knowledge (instead of assuming that the solution space is ergodic) and the solution does not represent pixels but coefficients. More advanced numerical techniques will certainly extend the possibilities of this method, which is currently mostly limited with bad quality and quantity of the observations.

Acknowledgements. I would like to thank Nikola Božinović (Institute for Space Physics, Boston University) for great help with the telescope equipment during the observations. I am also grateful to Igor Smolić (Petnica Science Center, Department for Astronomy) for precious comments and suggestions, as well as for providing reference 30. All the numerical algorithms were programmed in MatLab package, kindly provided by the Petnica Science Center.

References

*B*arucci *et al*. 1992. Ground based Gaspra modeling: comparison with the first Galielo image, Astronomy&Astrophysics, **266**: 385.

Birch P.V., Taylor R.C. 1989. Lightcurves and pole position of asteroid 3 Juno, Astronomy&Astrophysics Supplement Series, **81**: 409.

Bronsteyn V.A. 1982. *Planeti i ikh nablyudenie*. Moskva: Nauka

De Angelis G. 1993. A method to determine asteroid poles. *LPSC*, XXIV: 385.

Di Martino M., Zappala V., De Sanctis G., Cocciatoni I. Photoelectric Photometry of 17 Asteroids. *Icarus*, **69**: 338.

Dotto *et al*. 1995. Pole orientation and shape of 12 asteroids. *Icarus,* **117**: 313.

Harris A.W. 1987. Fourier analysis of asteroid lightcurves: some preliminary results. *LPSC*, XVIII: 385.

Harris A.W. *et al*. 1989. Photoelectric observations of asteroids 3, 24, 60, 261, and 863. *Icarus*, **77:** 177.

Lagerros J. S. V. 1996. New thermal model of asteroids IV, *Astronomy&Astrophysics,* **310**: 1011.

Lagerros J.S.V. 1997. New thermal model of asteroids V, Astronomy&Astrophysics, **325**: 1226.

Kaasalainen M., Lamberg L., Lumme K., Bowell E. 1992. Interpretation of lightcurves of atmosphereless bodies. *Astronomy&Astrophysics*, **259**: 318.

Karttunen H. 1989. Modelling asteroid brightness variations I, Astronomy&Astrophysics, **208**: 314.

Karttunen, H., Bowell, E. 1989. Modelling asteroid brightness variations I. *Astronomy&Astrophysics,* **208**: 320.

Krugly *et al*. 1994. Asteroid 83 Beatrix – photometry and model. *Astronomy&Astrophysics*, Supplement Series, **104**: 143.

Kwiatkowski T. 1995. Sidereal period, pole and shape of asteroid 1620 Geographos. Astronomy&Astrophysics, **294**: 274.

Lagerkvist C.-I., Magnusson P. 1990. Analysis of asteroid lightcurves II, Astronomy&Astrophysics, **243**: 512.

Licandro J., Gallardo T., Tancredi G. 1994. Lightcurves and pole determinations for the asteroids 31 Euphrosyne, 196 Phylomena and 471 Papagena, Revista Mexicana de Astronomia y Astrofisica, **28**: 91.

Lumme K., Karttunen H., Bowell E. 1989. A spherical harmonics method for asteroid pole determination. *Astronomy&Astrophysics,* **229**: 228.

Karttunen H., Muinonen K. 1991. Error analysis of lightcurve periods. *Astronomy&Astrophysics*, **242**: 513.

Magnusson P. 1991. Analysis of asteroid lightcurves III. *Astronomy&Astrophysics*, **243**: 512.

Magnusson *et al*. 1996. Photometric observations and modeling of asteroid 1620 Geographos. *Icarus*, **123**: 227.

Magnusson *et al*. 1997. Physical model of near-Earth asteroid 6489 Golevka (1991 JX) from optical and infrared observations. *The Astronomical Journal,* **114** (3): 1234.

Martinez P., Klotz A. 1998. *A practical guide to CCD astronomy*. Cambridge Univesity Press

Mecke K.R. 2000. Additivity, complexity and beyond: Applications of Minkowski functionals in statistical physics. *Mathematische Annalen*, **119:** 111

Minor Planet Ephemeris Service, Minor Planet Center. cfa-www.harvard.edu/iau/ephemerides.

Minkowski H. 1903. *Matematische Annalen*, **4:** 34.

Muinonen K., Lagerros J. S. V. 1998. Inversion of shapes of irregular solar system bodies. *Astronomy&Astrophysics*, **333**: 753.

Pospieszalska-Surdej A., Surdej J. 1985. Determination of the pole orientation of an asteroid. The amplitude-aspect relation revisited. *Astronomy&Astrophysics*, **149**: 186.

Press W.H., Teukolsky S.A., Vetterling W.T., Flannery B.P. 1997. *Numerical Recipes in C: The Art of Scientific Computing*. Cambridge University Press

Rowe B. H. 1993. Calculating Asteroid Diameters. *Sky&Telescope*, (June 1993): 83

Russel H. N. 1906. On the light-variations of asteroids and satellites. *Astrophysical Journal,* XXIV (1): 1.

Schroll A., Schober H. J., Lagerkvist C.-I. 1981. Evidence for Color Variations on the Surface of 3 Juno: New Photoelectric UBV-Observations. *Astronomy&Astrophysics,* **104**: 269.

Schober H.J., Schroll A. 1982. Color variations of asteroids during rotation. In: *Sun and planetary system*. Dordrecht: D. Reidel Publishing, pp. 285-6.

Simonenko A. 1985. *Asteroidi*. Moskva: Nauka.

Tancredi G., Gallardo T. 1990. A comparison of two pole determination methods for the asteroids, *Astronomy&Astrophysics,* **242**: 279.

Tycho 2 Star Catalogue

Uppsala Photometric Catalogue of Asteroids. *1995*.

Uppsala Catalogue of Spin Vectors of Asteroids. *1995*.

Zappala V., Cellino A., Barucci A. M., Fulchignoni M., Lupishko D. F. 1990. Analysis of amplitude-phase relationship among asteroids. *Astronomy&Astrophysics,* **231:** 548.

Mihailo Čubrović

Fizičke karakteristike i fotogrametrijska analiza oblika asteroida 3 Juno

Dat je model asteroida 3 Juno urađen na osnovu krivih sjaja u vidljivoj svetlosti. Metod modeliranja bazira se pre svega na fotomorfografskom metodu (Kaasalainen *et al*. 1992). Za modeliranje je korišćeno petnaest krivih sjaja, od kojih je jedna snimljena u ISP i ovde prvi put objavljena, dok su ostale preuzete iz Uppsala fotometrijskog kataloga asteroida.

Sve krive su obrađene Furijeovom analizom, čime je dobijena vrednost perioda. U prvoj aproksimaciji asteroid je posmatran kao troosni elipsoid čiji su parametri odnosi poluosa a/b i a/c, a koordinate pola β_o i λ_o. Ovi parametri su određeni kombinacijom modifikovanih relacija amplituda-nagibni ugao i metoda sfernih harmonika (Karttunen *et al*. 1989). Tako dobijeni parametri su iskorišćeni kao početna vrednost pri modeliranju fotomorfografskim metodom. Oblik se kod ovog metoda opisuje standardnim formalizmom diferencijalne geometrije, i dobija se kao Gausova površinska gustina u funkciji koordinata. Modeliranje je izvršeno sa nekoliko zakona odbijanja (Lomel-Zeligerov, Lume-Bauelov i njihove kombinacije). Kao numerički metod za inverziju Fredholmove integralne jednačine prve vrste koja sadrži Gausovu površinsku gustinu kao nepoznatu funkciju, iskorišćen je modifikovani metod maksimizacije entropije. Ovaj metod je, za razliku od standardne tehnike statističke inverzije, omogućio ispitivanje lokalnih nekonveksnosti i nehomogenosti površine, kao i veću stabilnost rešenja.

Dobijeni vektor rotacije Juna je $\beta_o = 36 \pm 6°$, $\lambda_o = 104 \pm 4°$, $P = (0.300396 \pm \pm 0.000002)$ d. Model je prikazan na slikama 4-9, u šest normalnih projekcija. Modeli dobijeni sa različitim zakonima odbijanja se razlikuju samo po malim lokalnim strukturama, koje su najvećim delom u granicama greške. Najveća struktura, vidljiva pri dnu slika 6 i 7, je konkavna oblast sa nešto nižim albedom od ostatka površine koja možda predstavlja udarni krater. Ostale varijacije albeda su verovatno u granicama greške, pa se ne mogu razmatrati.

Dobijeni rezultat je ohrabrujući i ukazuje na potencijalno veliku količinu informacija koja se može rekonstruisati fotomorfografijom. Najvažnija ograničenja su količina i kvalitet posmatranja i numeričke tehnike. Može se pretpostaviti da će se po oba pitanja u budućnosti napredovati, pa se od modeliranja na osnovu krivih sjaja mogu očekivati korisne informacije o fizičkim osobinama asteroida.